An Air Stagnation Index to Qualify Extreme Haze Events in Northern China

JIN FENG

Institute of Urban Meteorology, China Meteorological Administration, Beijing, China, and National Center for Atmospheric Research, Boulder, Colorado

JIANNONG QUAN

Institute of Urban Meteorology, China Meteorological Administration, Beijing, China

HONG LIAO

Jiangsu Key Laboratory of Atmospheric Environment Monitoring and Pollution Control, Collaborative Innovation Center of Atmospheric Environment and Equipment Technology, School of Environmental Science and Engineering, Nanjing University of Information Science and Technology, Nanjing, China

YANJIE LI

State Key Laboratory of Numerical Modeling for Atmospheric Sciences and Geophysical Fluid Dynamics, Institute of Atmospheric Physics, Chinese Academy of Sciences, Beijing, China

XIUJUAN ZHAO

Institute of Urban Meteorology, China Meteorological Administration, Beijing, China

(Manuscript received 27 November 2017, in final form 18 June 2018)

ABSTRACT

Stagnation weather affects atmospheric diffusion ability, and hence causes the occurrence of haze events, which have been happening frequently in northern China (NC). This work puts forward an air stagnation index (ASI_{TS}) to characterize the stagnation weather in NC, in which the processes of ventilation, vertical diffusion, and wet deposition potency are concerned. ASI_{TS} can be applied to analyze air stagnation conditions with daily to monthly time scale. It is shown that the ASI_{TS} and particulate matter smaller than 2.5 μm in diameter ($PM_{2.5}$) concentrations own similar lognormal probability distribution functions on both daily and monthly time scales. And the correlation analyses between the ASI_{TS} and $PM_{2.5}$ concentrations indicate that the ASI_{TS} can reflect the monthly and daily variations in $PM_{2.5}$ concentrations in NC. In addition, ASI_{TS} could be used as a leading predictor of haze events since correlation coefficients of ASI_{TS} leading $PM_{2.5}$ concentrations by 1 day were significant and were larger than simultaneous correlation coefficients in almost all areas in NC. The robust relationship between ASI_{TS} and $PM_{2.5}$ concentrations exists possibly because the index can reflect the activities of synoptic systems. ASI_{TS} could be a useful statistical indicator for variations in $PM_{2.5}$ concentrations and haze events, and a good tool in analyzing the relationship between climate change and long-term variations in haze in NC.

1. Introduction

Northern China (NC; Fig. 1) has been experiencing severe air pollution during recent years because of high quantities of emissions accompanied by rapid economic development and urbanization (Hu et al. 2014; IPCC 2013; Mijling et al. 2013; Tie et al. 2009; Yuxuan Wang et al. 2013; Zhang et al. 2012). Aerosol concentrations over NC are highly sensitive to meteorological parameters and show strong variabilities at daily (Quan et al. 2014; Guo et al. 2017), monthly (Zhang et al. 2012; Guo et al. 2017), and annual time scales (Mu and Liao 2014; Feng et al. 2016) since the meteorological factors, including wind speed, planetary boundary layer height (PBLH), and precipitation, can modulate aerosol dilution, transport,

Supplemental information related to this paper is available at the Journals Online website: https://doi.org/10.1175/JAS-D-17-0354.s1.

Corresponding author: Jin Feng, jfeng@ium.cn

DOI: 10.1175/JAS-D-17-0354.1

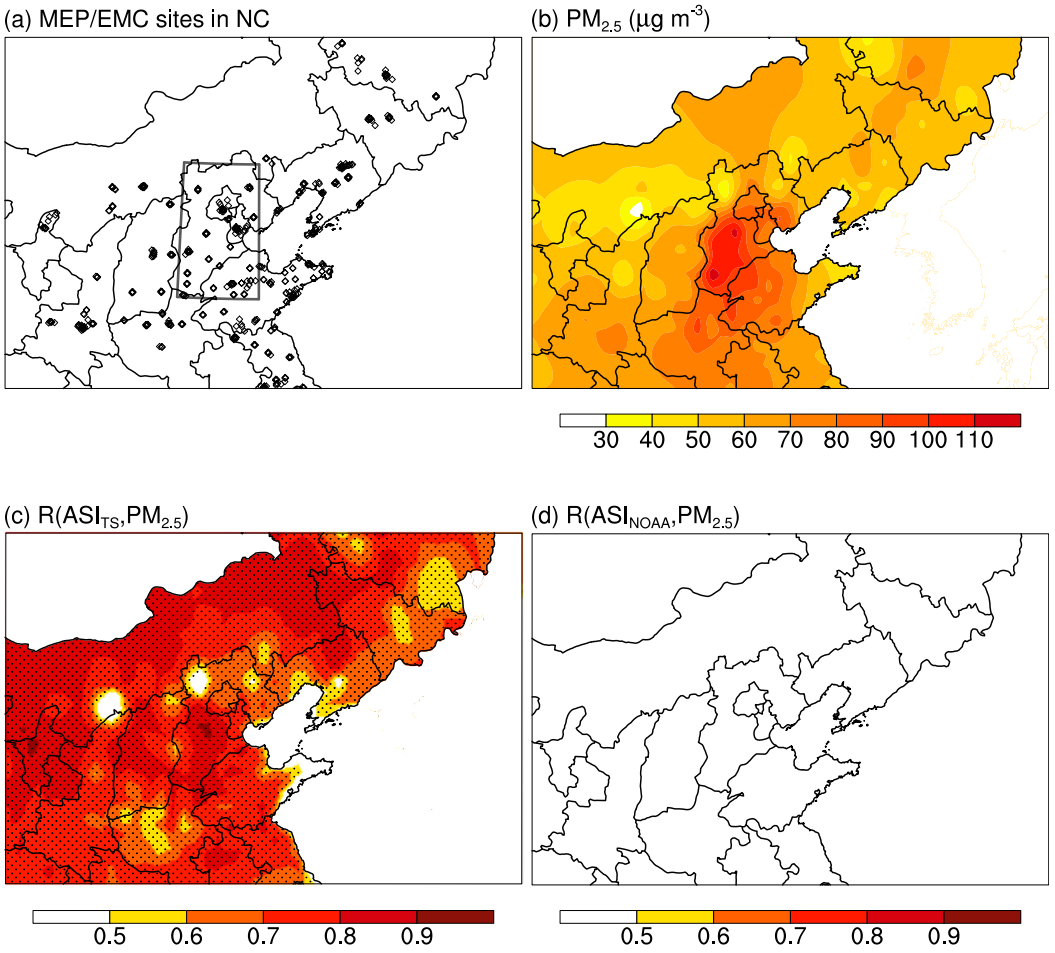

FIG. 1. (a) Geographic distribution of the observation sites (diamonds) for the observed $PM_{2.5}$ concentrations in NC (32°–47°N, 105°–132.5°E, including north China, northeast China, and their near areas in the manuscript). The polygon represents the BTH region (36°–42°N, 114°–118.5°E). (b) Time-averaged $PM_{2.5}$ concentrations in 0.625° × 0.5° grids obtained via interpolation from 1 Apr 2013 to 31 Mar 2016. (c),(d) The geographic distributions of correlation coefficients between the monthly mean ASI_{TS} values and $PM_{2.5}$ concentrations and ASI_{NOAA} values and $PM_{2.5}$ concentrations, respectively, in NC from 1 Apr 2013 to 31 Mar 2016. The dots in (c) and (d) denote areas statistically passing the 99% confidence level. The observed $PM_{2.5}$ data are from the China National EMC published by the MEP.

deposition processes, and even chemical reactions (Mu and Liao 2014; Seinfeld and Pandis 2006; Zhao et al. 2012). Hence, meteorology plays an important role in the occurrence of extreme haze events, characterized by extremely high concentrations of particulate matter smaller than 2.5 μm in diameter ($PM_{2.5}$) (Quan et al. 2011; Zhao et al. 2013; R. Zhang et al. 2014; Guo et al. 2015; Wang et al. 2015; Gao et al. 2016). Under favorable meteorological conditions, $PM_{2.5}$ can rapidly accumulate to very high levels. For example, Quan et al. (2014) reported a wave of haze events over the North China Plain (NCP) with a maximal observed $PM_{2.5}$ concentration reaching 600 $\mu g\,m^{-3}$ and a sustained haze event even persisted up to 6 days in Beijing during December 2012. They indicated that stagnation weather, generally characterized by low wind speeds and decreased PBLH, was the dominant factor in these haze events.

It is desired to establish a single "meteorological index" that could qualify the relationship between variations in meteorology and aerosol concentrations. It could be useful to understand the impacts of variations in weather and climate on the air quality, and to predict the occurrences of haze events. However, it is a very difficult issue to make a uniform index to trace the evolution of aerosol concentrations in any region and time scale because the interactions between aerosols and multimeteorological factors are extremely complex, even with many unclear mechanics, especially on the diurnal time scale (Z. Li et al. 2017). Hence, a meteorological index should have its focused spatial and

TABLE 1. Meteorological indices used for qualifying variations in the aerosol concentrations or air quality from previous studies in NC.

Meteorological index scheme	Method/definition	Applied time scale	Involved subregions in NC
Horton et al. (2014) (ASI_{NOAA})	Percentage of stagnation days in a period of time, where stagnation days are defined by thresholds of meteorological parameters	Greater than or equal to monthly	All of NC
Feng et al. (2016)	Multilinear regression with eight meteorological parameters in each grid cell	Interannual	Central and southern NC
Yang et al. (2016)	Tendency of wet equivalent potential temperature of air masses to compare with the variations in visibility	Less than or equal to daily	Central and southern NC
Cai et al. (2017)	Summation of three normalized atmospheric factors selected by statistical correlation	Daily	Vicinity of Beijing
Huang et al. (2017)	Modified ASI_{NOAA} with a topographically dependent upper-air wind speed and without concerning the criterion of temperature inverse	Greater than or equal to monthly	All of NC

temporal scope. These meteorological indices that were applied to NC in previous studies are presented in Table 1. In summary, two methods were used to establish these indices. The first and most common one is to establish an empirical–statistical model using $PM_{2.5}$ concentrations and multivariable meteorological data by multilinear regression (MLR; Tai et al. 2010, 2012; Feng et al. 2016) or through other statistical methods, such as the summation of multinormalized atmospheric factors (Cai et al. 2017). An empirical–statistical meteorological index is efficient for studying variations at a specific place and time scale but it lacks a sufficient physical background. The application scopes of these indices are narrow. The second method is to establish an index that can physically characterize the air stagnation weather, which is strongly related to the variability in aerosol concentrations (Jacob and Winner 2009; Sun et al. 2013; Ye et al. 2016).

The air stagnation index (ASI) was issued by the National Oceanic and Atmospheric Administration (NOAA) in the United States (https://www.ncdc.noaa.gov/societal-impacts/air-stagnation/overview). Here we refer to it as the ASI_{NOAA}, which was also referred to as NCDC ASI in Horton et al. (2012, 2014). ASI_{NOAA} is defined as the percentage of stagnation days in a period of time (e.g., 1 month). Stagnation days herein refer to days in which the daily sea level geostrophic wind speed is less than $8\,m\,s^{-1}$ (or when the surface wind speeds are less than $4\,m\,s^{-1}$, or the wind speed at 10 m is less than $3.2\,m\,s^{-1}$), on which the daily wind speed at 500 hPa is less than $13\,m\,s^{-1}$, and on which no precipitation occurs and the daily temperature is inverted within the PBL (using the layer between the surface and 850 hPa in practice). By the definition, the ASI_{NOAA} scheme mainly involves three key processes related to variations in aerosol concentrations: 1) local horizontal ventilation in the atmospheric column, that is, ventilation potency, 2) local vertical diffusion potency in the PBL, and 3) wet deposition potency. The ASI_{NOAA} has been widely used in many studies in many regions of the world (Leibensperger et al. 2008; Horton et al. 2012, 2014), including China (Huang et al. 2017). And it is reportedly able to characterize the seasonal and interannual variations in aerosol pollution (Mamtimin and Meixner 2011). However, it is worthy to note that the ASI_{NOAA} is semiempirical based on observations in the United States (Korshover 1976; Korshover and Angell 1982; Wang and Angell 1999), and thus it could not be suitable for capturing the haze event effectively in other regions. For example, the criterion of temperature inverse in the definition of ASI_{NOAA}, which only uses two pressure levels, could not be applicable in China because the temperature profiles in the low troposphere, including the PBL, seem extremely complex in China because of the strong positive feedback induced by high aerosol concentrations (Yuan Wang et al. 2013; Guo et al. 2016; Z. Li et al. 2017). According to Cai et al. (2017), only 28% of the severe haze events in Beijing were captured using the ASI_{NOAA}. In addition, the ASI_{NOAA} cannot reflect short-term variations in aerosol concentrations because of its representation of stagnation days as percentages in a given period of time.

To fill these gaps, considering the basic aerosol processes related to meteorological fields, we introduced a new ASI scheme (hereafter referred to as ASI_{TS}) that is applicable to daily and monthly variations in aerosol concentrations in NC. This paper is organized as follows. An illustration of the ASI_{TS} scheme, the meteorological data, and the observed $PM_{2.5}$ concentrations are provided in section 2. In section 3, we demonstrate the geographic distribution and probability distribution function (PDF) of ASI_{TS} and the performance of ASI_{TS} in capturing the monthly variations in $PM_{2.5}$ concentrations over NC, which are accompanied by a comparison of ASI_{TS} with the ASI_{NOAA}. Then we apply the ASI_{TS} to the daily $PM_{2.5}$ concentration variations and prediction of extreme haze occurrence in NC. We also

discuss the uncertainties in the relationship between ASI_{TS} and the $PM_{2.5}$ concentrations induced by the scheme parameters of ASI_{TS}. Finally, in section 4, we draw our conclusions and discuss the potential applications of ASI_{TS}.

2. Data and methods

a. *The scheme of ASI_{TS}*

The ASI_{TS} scheme is designed to include the same three basic processes that strongly effect stagnation weather conditions and the accumulation of aerosols over NC as ASI_{NOAA}, with a form of

$$ASI_{TS} = P_V P_D P_W, \tag{1}$$

where P_V, P_D, and P_W represent the ventilation potency, vertical diffusion potency in the PBL, and wet deposition potency, respectively. In this index, the three parameters are multiplied together rather than added to avoid determination of the weights of the three parameters, which could vary in different circumstances. This method was used in many parameterization schemes in models and remote sensing retrieval of aerosols (Chen et al. 2012; Seinfeld and Pandis 2006; Tang et al. 2017; Zhang and Li 2015). As a result, the ASI_{TS} series always has the same time resolution as the meteorological samples used in the right-hand terms. In addition, several mathematic processes are adopted to make ASI_{TS} dimensionless and keep its value not exceeding two orders of magnitude (similar to the variation of $PM_{2.5}$), which are detailed in the following paragraph.

In the ASI_{TS} scheme P_V presents the effects of the wind speed in the local atmospheric column, rather than only surface winds in the ASI_{NOAA}, which are simply represented by the weighted average of the wind speed from the surface layer to the top of the atmosphere as follows:

$$\overline{U} = \frac{\int_{z_0}^{z_T} \sigma(z) U(z)\, dz}{\int_{z_0}^{z_T} \sigma(z)\, dz}, \tag{2}$$

where $\overline{U}$ denotes the weighted average of the wind speed, z_0 and z_T are the geopotential heights at the surface and the top of the atmospheric column, respectively, $U(z)$ is the wind speed at the geopotential height z, and $\sigma(z)$ denotes the weights of $U(z)$, thereby reflecting the independent impacts of the wind speed at a height z on the $PM_{2.5}$ concentrations at the surface. The vertical distribution of $\sigma(z)$ is difficult to determine at present. Since aerosols are basically concentrated in the PBL and decrease rapidly above the PBLH (Hara et al. 2011; Li and Han 2016), we assume well-mixed atmospheric conditions with confined aerosol masses in the PBL (Li et al. 2016; He et al. 2016). Then, the vertical distribution of $\sigma(z)$ is constant, and (2) can be simplified as

$$\overline{U} = \frac{1}{z_{PBL} - z_0} \int_{z_0}^{z_{PBL}} U(z)\, dz, \tag{3}$$

where z_{PBL} is the geopotential height at the top of the PBL. Some previous studies also labeled the term $\int_{z_0}^{z_{PBL}} U(z)\, dz$ in (3) the ventilation index (VI), which was found to be significantly negatively correlated with aerosol concentrations in China (Jiang et al. 2015; Liu et al. 2015). Therefore, P_V can be presented by the expression $P_V = f(\overline{U})$, where $f(\overline{U})$ is a decreasing function of $\overline{U}$. A simple expression of $f(\overline{U})$ can be written in form of the power law relationship $f(\overline{U}) = \lambda_V^{-1}\overline{U}^{-\alpha}$, where $\alpha > 0$, to illustrate the nonlinear relationship between wind speed and the $PM_{2.5}$ concentrations (Liu et al. 2007; Cobourn 2010; You et al. 2016). In addition, the magnitude of $\overline{U}$ over NC has a wide range from 10^{-2} to $10^{1}\ m\ s^{-1}$ according to our calculations. Therefore, we set $\alpha = 1/4$ in order to keep the order of magnitude of P_V at 1 and to avoid excessively large values of P_V due to situations with very weak wind speeds in the PBL (i.e., $\overline{U} \to 0$). The uncertainty caused by the value of α in ASI_{TS} is discussed in section 3e. It is shown that α is not a sensitive parameter for the relationship between ASI_{TS} and $PM_{2.5}$ concentrations when $\alpha \le 1/2$ in NC. A scaling parameter λ_V, which is set to $1\ m\ s^{-1}$, also is used to make P_V dimensionless. Finally, P_V is expressed as follows:

$$P_V = \lambda_V^{-1}\left[\frac{1}{z_{PBL} - z_0}\int_{z_0}^{z_{PBL}} U(z)\, dz\right]^{-1/4}. \tag{4}$$

The parameter of vertical diffusion potency P_D depends on local turbulence characteristics. It is difficult to accurately describe mixing in the PBL by solving the underdetermined system of dynamic equations for turbulence (Lin and McElroy 2010). However, since aerosol masses are mainly concentrated in the PBL (Hara et al. 2011; Li and Han 2016), the PBLH can reflect the vertical diffusion capability. Hence, P_D is expressed as follows:

$$P_D = \frac{\lambda_D}{z_{PBL} - z_0}, \tag{5}$$

where λ_D is the scaling parameter for P_D. Because the order of magnitude of the PBLH is $\sim 10^3$ m over NC, λ_D is set to 10^3 m to confine the order of magnitude of P_D to 1.

The wet deposition is very efficient for the removal of aerosol masses. Hence, the precipitation threshold of $1\ mm\ day^{-1}$ used in the ASI_{NOAA} (Horton et al. 2012, 2014;

Huang et al. 2017) is reserved in the definition of P_W. Since P_W should be positive to avoid a singularity in the $\mathrm{ASI_{TS}}$ time series, P_W is expressed as follows:

$$P_W = e^{[1-\delta(r)]}, \tag{6}$$

where r is the daily mean accumulated precipitation rate (mm $\mathrm{day^{-1}}$) and

$$\delta(r) = \begin{cases} 1, & r \geq 1 \\ 0, & r < 1 \end{cases}. \tag{7}$$

The order of magnitude of P_W is also 1, similar to the P_V and P_D. The expression of P_W represents a significant decrease (e-folding) of the stagnation conditions due to precipitation.

Substituting (3), (4), and (6) into (1), the $\mathrm{ASI_{TS}}$ can be represented as follows:

$$\mathrm{ASI_{TS}} = \frac{\lambda e^{[1-\delta(r)]}\left[\dfrac{1}{z_{\mathrm{PBL}} - z_0}\displaystyle\int_{z_0}^{z_{\mathrm{PBL}}} U(z)\,dz\right]^{-1/4}}{z_{\mathrm{PBL}} - z_0}, \tag{8}$$

where $\lambda = \lambda_D/\lambda_V = 10^3$ s, which keeps the $\mathrm{ASI_{TS}}$ dimensionless, is a linear parameter that cannot impact the relationship between $\mathrm{ASI_{TS}}$ and $\mathrm{PM_{2.5}}$. Since P_V, P_D, and P_W are all positive and with an order of magnitude of 1, the $\mathrm{ASI_{TS}}$ will be positive and also has an order of magnitude of 1.

The $\mathrm{ASI_{TS}}$ scheme owns several favorable characteristics when compared with other previous indices: 1) the $\mathrm{ASI_{TS}}$ scheme does not include statistic–empirical parameters to represent the effects of meteorological variables and characterize the stagnation weather; 2) the $\mathrm{ASI_{TS}}$ scheme can be applied to the variations in $\mathrm{PM_{2.5}}$ concentrations on daily to monthly time scales (see section 3); and 3) $\mathrm{ASI_{TS}}$ is calculated with the same frequency of meteorological variables.

b. $PM_{2.5}$ data

The observed surface $\mathrm{PM_{2.5}}$ concentrations in NC are published by the China Ministry of Environmental Protection Environmental Monitoring Center (MEP/EMC) (http://113.108.142.147:20035/emcpublish/). The datasets became available in January 2013 when the MEP began to release real-time $\mathrm{PM_{2.5}}$ data. This study used daily and monthly averaged $\mathrm{PM_{2.5}}$ concentrations from 1 April 2013 to 31 March 2016 at approximately 472 sites in NC (Fig. 1a; 32°–47°N, 105°–132.5°E). In addition, we obtained the gridded $\mathrm{PM_{2.5}}$ data by spatially interpolating the original MEP observation sites into the meteorological data grid (0.625° × 0.5°; see section 2c) to avoid a heterogeneous distribution of observation sites and missing values at many sites. Such an approach was used in previous studies that analyzed the influences of meteorological factors on aerosol concentrations (Tai et al. 2010, 2012; T. Zhang et al. 2016). It should be noted that interpolation errors exist in areas where the $\mathrm{PM_{2.5}}$ observation sites are scarce, including northern Inner Mongolia and some mountainous areas in southwestern NC. Thus, analysis hereinafter will avoid these areas. Figure 1b shows the geographic distribution of the time-averaged $\mathrm{PM_{2.5}}$ concentrations by interpolating the observed data over NC from 1 April 2013 to 31 March 2016. The $\mathrm{PM_{2.5}}$ concentrations are the highest in the central and southern parts of the Beijing–Tianjin–Hebei region (BTH), up to 110–120 $\mu\mathrm{g\,m^{-3}}$, which is corresponding to the previous studies (Li et al. 2016; Zou et al. 2017). Some other areas in NC including the western Shandong Province, central Henan Province, central Shanxi Province, and the vicinity of Harbin had the mean $\mathrm{PM_{2.5}}$ concentrations of 90–100, 90–100, 70–80, and 70–80 $\mu\mathrm{g\,m^{-3}}$, respectively, which were also reported in previous studies (Quan et al. 2011; Zhang et al. 2012).

c. Meteorological data

The meteorological data, including the geopotential height, PBLH, and precipitation, come from the Modern-Era Retrospective Analysis for Research and Applications, version 2 (MERRA-2), dataset, which is available from the Goddard Earth Sciences Data and Information Services Center (GES DISC, https://disc.sci.gsfc.nasa.gov). The highest-resolution datasets (0.625° × 0.5°) in MERRA-2 are used to retrieve accurate interpolation results. The MERRA-2 meteorological datasets assimilated conventional and satellite observations detailed in Koster et al. (2016) and Gelaro et al. (2017), and were validated in Bosilovich et al. (2015). Compared with the National Centers of Environmental Prediction–Department of Energy AMIP-II reanalysis (NCEP-2) data, the normalized mean bias of geopotential height and wind speed in the low troposphere in NC (lower than 500 hPa) were 0.1% and 7%, respectively. Reichle et al. (2017) assessed the seasonal biases and time series correlation of the MERRA-2 dataset versus the Global Precipitation Climatology Project, version 2.2 (GPCPv2.2), precipitation dataset over 1980–2015 and showed that the MERRA-2 precipitation data have no apparent bias over NC. MERRA-2 data have been used in many studies on the structure and the dynamics of atmospheric circulation systems (Coy et al. 2016; Bosilovich et al. 2017) and the global atmospheric water balance and variability (Bosilovich et al. 2017). In this manuscript, the $\mathrm{ASI_{TS}}$ is calculated using the MERRA-2 data from 1 April 2013 to 31 March 2016. Besides the original gridded MERRA-2 data, we also use the sites' data that are obtained via bilinear interpolation from the corresponding gridded data into the $\mathrm{PM_{2.5}}$ monitoring network of the MEP/EMC.

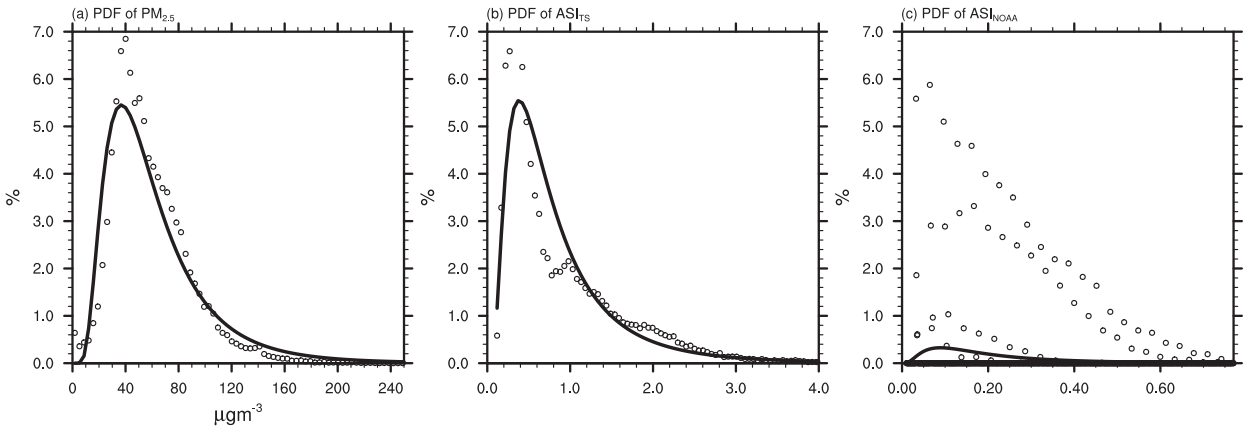

FIG. 2. The PDFs (circles) and their lognormal fitting curves (solid lines) for the monthly averaged (a) $PM_{2.5}$, (b) ASI_{TS}, and (c) ASI_{NOAA} values in NC, obtained from the MEP $PM_{2.5}$ observations from April 2013 to March 2016.

3. Results and analysis

a. *The monthly variations of ASI_{TS} in NC*

ASI_{TS} had a robust relationship with the monthly variations in $PM_{2.5}$ concentrations in NC. Figure 1c is the spatial distribution of correlation coefficients between the monthly ASI_{TS} and $PM_{2.5}$ concentrations in the same grid. It is shown that the monthly variations in ASI_{TS} are correlated positively with $PM_{2.5}$. The correlation coefficients in 99.1% of the areas in NC passed the *t* test at a 99% confidence level. The correlation coefficients in BTH, Shanxi, and the northern Anhui Province were large and reached up to 0.9–1.0, 0.8–0.9, and 0.8–0.9, respectively. Since these regions were also the severe aerosol-polluted regions in NC (Fig. 1b), it is suggested that the high aerosol pollution levels in these areas should be largely attributed to the air stagnation conditions. In addition, we also show the geographic distribution of correlation coefficients between the monthly ASI_{NOAA} values and $PM_{2.5}$ concentrations in NC (Fig. 1d). It is clear that the ASI_{TS} shows a more significant relationship with $PM_{2.5}$ concentrations than the ASI_{NOAA} among the grid cells throughout NC, indicating that the ASI_{TS} is more suitable for analyzing monthly variations of $PM_{2.5}$ concentrations in NC than the ASI_{NOAA}.

To conduct a more in-depth analysis of these relationships, the PDFs of the ASI_{TS}, ASI_{NOAA}, and the $PM_{2.5}$ concentrations are shown in Fig. 2. The PDF of the monthly $PM_{2.5}$ concentrations in NC was a smooth lognormal distribution (Fig. 2a), with the highest probability density at approximately 41 $\mu g\,m^{-3}$. The lognormal PDF distribution of $PM_{2.5}$ concentrations is similar to the results from previous studies (Šakalys et al. 2004; Ovadnevaitė et al. 2007; Lu 2002). We calculate the normalized mean bias [NMB; $\mathrm{NMB} = \sum_{c=0}^{C_{\max}} |P(C) - P_{\mathrm{LN}}(C)| / \sum_{c=0}^{C_{\max}} P_{\mathrm{LN}}(C) \times 100\%$, where C represents the $PM_{2.5}$ concentrations, and $P(C)$ and $P_{\mathrm{LN}}(C)$ are the probability values of the observed concentration C and the lognormal fitting PDF curve, respectively] of the $PM_{2.5}$ to compare the similarities between the PDF of the $PM_{2.5}$ concentrations and its lognormal fitting curve. The NMB of the $PM_{2.5}$ concentrations toward its lognormal function curve was 24.0%. By comparison, the PDF of the monthly ASI_{TS} values was also smooth and showed a favorable lognormal distribution similar to the PDF of the $PM_{2.5}$ concentrations (Fig. 2b). The NMB of the ASI_{TS} PDF toward its lognormal function curve was 27.4% (the NMB here is the same as the equation for $PM_{2.5}$ concentrations but the value of C is ASI_{TS}), which was similar to the NMB of the $PM_{2.5}$ (24.0% in Fig. 2a) and was much better than that of the ASI_{NOAA} (179.1% in Fig. 2c), further indicating that the ASI_{TS} can better reflect the monthly $PM_{2.5}$ variations in NC than ASI_{NOAA}.

Considering that the BTH is the most polluted area in NC (Fig. 1b), we particularly compare the monthly variations in the regional-mean ASI_{TS}, ASI_{NOAA}, and $PM_{2.5}$ in BTH from April 2013 to March 2016 (Fig. 3). It is clear that the ASI_{TS} scheme can capture the peaks and troughs of the monthly $PM_{2.5}$ concentration series, with a significant correlation coefficient of 0.86, which passes the *t* test at 99% confidence level. The ASI_{TS} had a clear seasonal fluctuation with high values from December to February (1.6–2.4) and low values from May to September (0.3–1.0). The simultaneous monthly mean $PM_{2.5}$ concentrations in BTH were 100–140 $\mu g\,m^{-3}$ from December to February and 30–50 $\mu g\,m^{-3}$ from May to September.

b. *The daily variations of ASI_{TS} in NC*

The ASI_{TS} scheme can also be applied to daily timescale variations, which is highly needed in analyzing haze events. Figure 4a shows the geographic distribution of correlation coefficients between the daily ASI_{TS} and

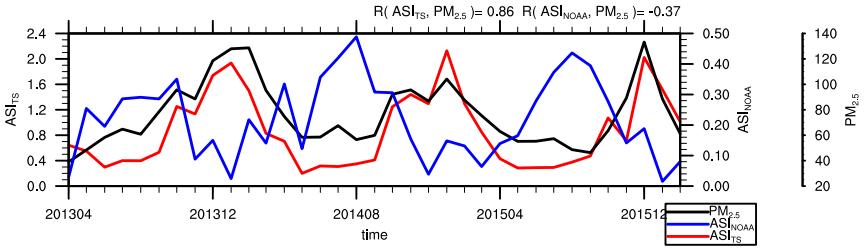

FIG. 3. The monthly mean $PM_{2.5}$ concentrations (black line; $\mu g\,m^{-3}$), and ASI_{TS} (red line) and ASI_{NOAA} (blue line) values in BTH from April 2013 to March 2016. The correlation coefficients between the $PM_{2.5}$ concentrations and the ASI_{TS} and ASI_{NOAA} are 0.86 and −0.37, respectively.

$PM_{2.5}$ concentrations in NC from 1 April 2013 to 31 March 2016. Among almost all of the NC grids, the daily ASI_{TS} and $PM_{2.5}$ concentrations showed a significant correlation. The correlation coefficients were 0.6–0.7 in BTH and 0.5–0.6 in the other areas with high $PM_{2.5}$ concentrations (as shown in Fig. 1b). In addition, similar to the monthly analyses, we also calculate the PDFs of the daily $PM_{2.5}$ concentrations and the daily ASI_{TS} (Figs. 4b and 4c, respectively). The PDFs of $PM_{2.5}$ and ASI_{TS} were lognormal distributions, with similar NMBs of 16.9% and 9.7%, respectively. These results indicate that the ASI_{TS} can also reflect the daily $PM_{2.5}$ variations in NC.

Furthermore, 10 urban observation sites at aerosol-polluted cities, including Beijing, Tianjin, Shijiazhuang, Xi'an, Zhengzhou, Yinchuan, Ji'nan, Taiyuan, Harbin, and Hohhot (marked in Fig. 4a), are selected to examine the relationship between the local ASI_{TS} and $PM_{2.5}$ concentrations. All those cities have been suffering heavy aerosol pollution reported by previous studies (Huang et al. 2011; Sun et al. 2013; Han et al. 2014; Mao et al. 2014; Wang et al. 2014; Q. Zhang et al. 2015; Gui et al. 2016; J. Li et al. 2017; Wang et al. 2017). The correlation coefficients between the daily ASI_{TS} and $PM_{2.5}$ at the 10 polluted cities range from 0.4 to 0.7 and pass the t test at a 99% confidence level, further indicating that the ASI_{TS} can be used to assess the $PM_{2.5}$ variations in polluted cities of NC.

To present the relationship between high ASI_{TS} and extreme haze, we define an extreme haze day (EHD) as the day with the 5% highest daily $PM_{2.5}$ concentrations during the period of the analysis (from 1 April 2015 to 31 March 2016 in Fig. 5). The high ASI_{TS} values essentially companied the occurrence of EHDs for the 10 cities (Fig. 5). Taking Beijing as an example, EHDs occurred mainly from October 2015 to March 2016 with maximum daily mean $PM_{2.5}$ concentrations of up to 200–500 $\mu g\,m^{-3}$, which is similar to the findings in previous studies (Gui et al. 2016; J. Li et al. 2017). The high ASI_{TS} values in the period also generally companied the EHDs, with the peak values ranging from 1.8 to 7.0. Two other BTH cities, Tianjin and Shijiazhuang, had a similar EHD occurrence as Beijing during the same period. The local ASI_{TS} values in the two cities ranged from 3.0 to 10.0 and also effectively captured the aerosol pollution episodes. In Xi'an, Yinchuan, Ji'nan, Taiyuan, and Hohhot, the EHDs in the wintertime were always accompanied by high ASI_{TS} values. It should be noted that the relationship between the daily $PM_{2.5}$ concentrations and ASI_{TS} may be interfered by other factors, including strong nonlocal aerosol mass transportation, emergency emission control measures, and accidental emissions from biomass burning in NC (C. Chen et al. 2015; Z. Chen et al. 2015; Yang et al. 2015; Long et al. 2016). For example, the ASI_{TS} scheme does not favorably track the two extreme events in Zhengzhou during January 2016, possibly because they were largely contributed by transportation from other places (Wang et al. 2017).

To present the close relationship between high ASI_{TS} and EHDs, Fig. 6 illustrates the ASI_{TS} PDFs for EHDs (daily $PM_{2.5}$ concentration $\geq 142\,\mu g\,m^{-3}$) and non-EHDs (daily $PM_{2.5}$ concentration $< 142\,\mu g\,m^{-3}$) in NC from 1 April 2013 to 31 March 2016. It is clear that the ASI_{TS} on EHDs and non-EHDs had substantially different values. Although these PDFs were lognormal (similar to those shown in Figs. 4b and 4c), the frequency of air stagnation weather in NC increased markedly on EHDs compared with non-EHDs, with a significant shift in ASI_{TS} toward higher values. The ASI_{TS} of highest probability density and mean ASI_{TS} values of EHDs were 1.3 and 2.5, respectively, greater than the values of non-EHDs (0.3 and 1.2, respectively). These results suggest that ASI_{TS} can qualify the occurrence of EHDs in NC.

c. *Application of ASI_{TS} as a predictor of extreme haze events*

Because air stagnation weather provides a favorable atmospheric environment for the accumulation of aerosol masses (Wang and Angell 1999), it is suggested that the effects of air stagnation weather on the $PM_{2.5}$ concentrations are not immediate but rather precede variations in the $PM_{2.5}$ concentrations. Hence, an ASI should have the ability to be a leading predictor of EHDs. To verify this assumption, Fig. 7 presents the

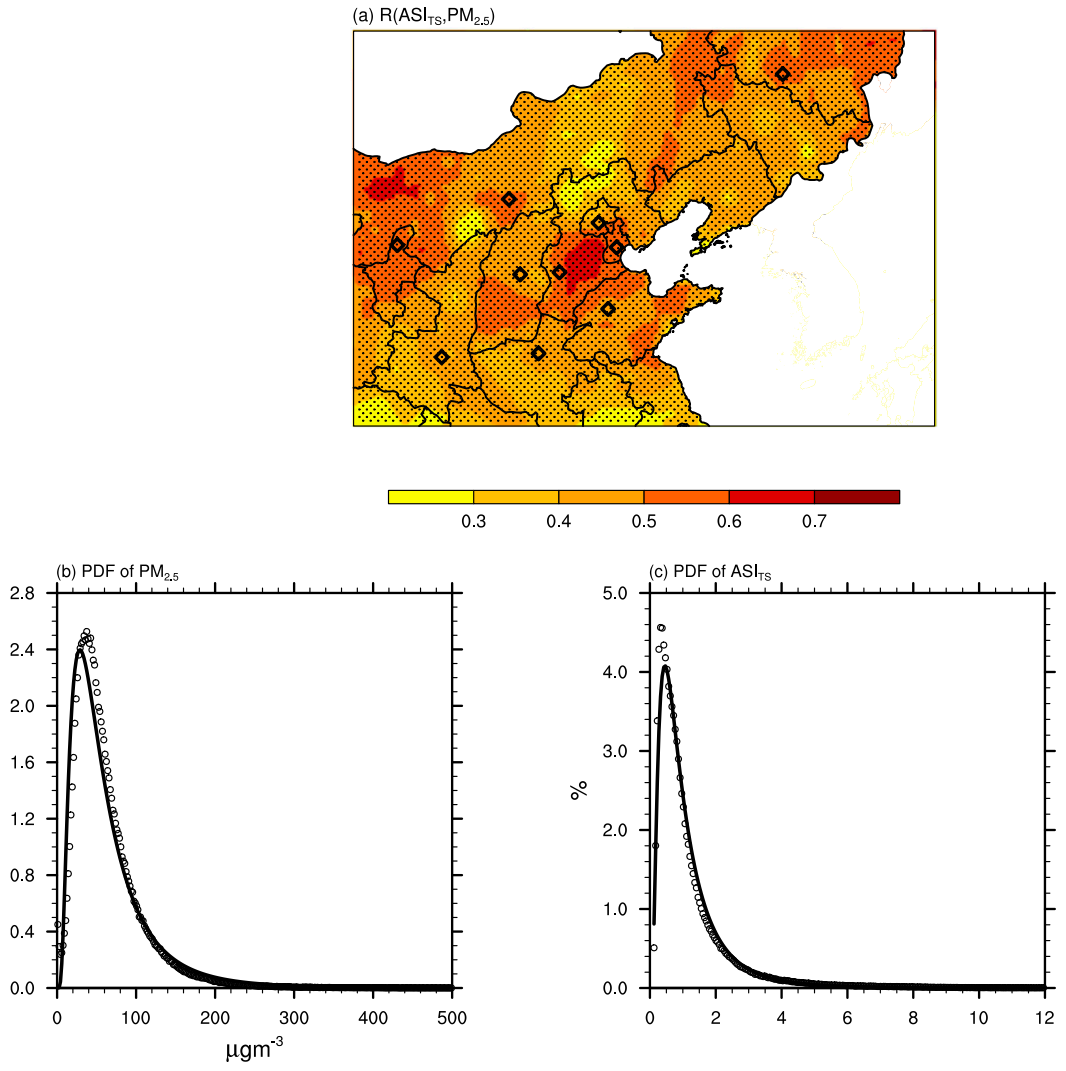

FIG. 4. (a) Geographic distribution of correlation coefficients between the daily ASI_{TS} values and the $PM_{2.5}$ concentrations in NC from 1 Apr 2013 to 31 Mar 2016. The dots denote areas statistically passing the 99% confidence level. The selected 10 aerosol-polluted cities with severe aerosol pollutions in NC are marked by black diamonds. (b),(c) The PDFs (circles) and their lognormal fitting profiles (black lines) for the daily $PM_{2.5}$ concentrations and ASI_{TS} values, respectively, in NC.

lead–lag correlation coefficients between the $PM_{2.5}$ concentrations and ASI_{TS} in the same 10 cities as shown in Fig. 5. It shows that the largest correlation coefficients between ASI_{TS} and the $PM_{2.5}$ concentrations were not simultaneous. Rather, ASI_{TS} led $PM_{2.5}$ concentrations by 1 day for all of the 10 cities, with the maximal significant lead–lag correlation coefficients ranging from 0.6 to 0.8. Significant lead correlation coefficients were also maintained for at least 4 days in each of the 10 cities as air stagnation days as defined by Wang and Angell (1999). Moreover, the correlation coefficients of ASI_{TS} leading $PM_{2.5}$ concentrations by 1 day were significant in all of the areas in NC and were larger than the simultaneous correlation coefficients in approximately 98% of the grid cells in NC (Fig. 8). In the severely polluted regions mentioned in section 2b, such as the southern BTH, the lead correlation coefficients reached up to 0.6–0.8. These results indicate that ASI_{TS} can reflect the aerosol mass accumulation and diffusion processes in NC.

At present, although various chemical transport models (CTMs) such as the WRF model with Chemistry (WRF-Chem; Chen et al. 2016), the Community Multiscale Air Quality (CMAQ) modeling system (Hu et al. 2016), and the Nested Air Quality Prediction Model System (NAQPMS; J. Li et al. 2017) have been used to

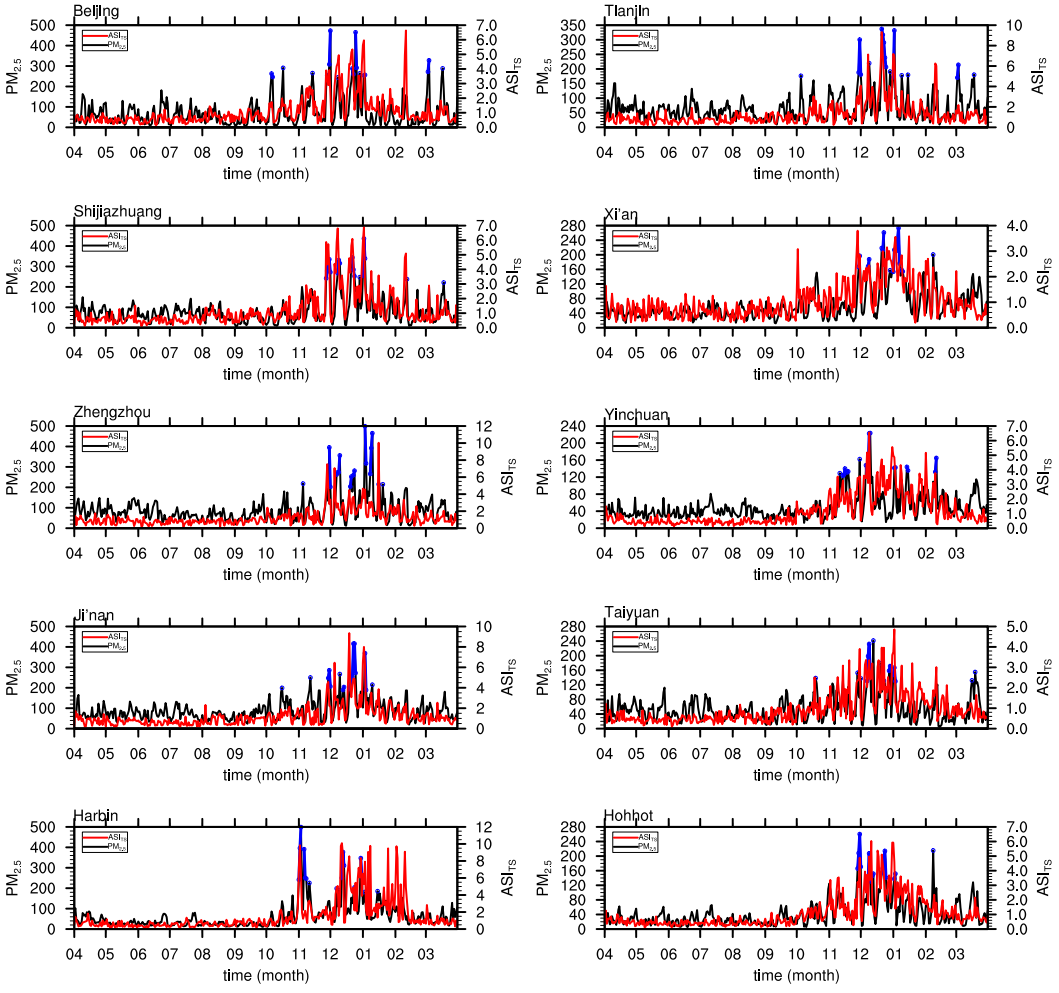

FIG. 5. $PM_{2.5}$ concentrations ($\mu g\,m^{-3}$) on non-EHDs (black lines) and EHDs (blue lines), and the ASI_{TS} values (red lines) for the selected 10 aerosol-polluted cities from Fig. 4a between 1 April 2015 and 31 Mar 2016.

forecast $PM_{2.5}$ concentrations in NC, extreme haze predictions have generated considerable uncertainties in NC due to the uncertainties in parameterization of physical and chemical processes and out-of-date emission inventory. The significant lead correlation between ASI_{TS} and the $PM_{2.5}$ concentrations indicate that the ASI_{TS} of the previous day should be able to predict the daily $PM_{2.5}$ concentrations and the occurrence of EHDs in NC. Hence, we establish a simple prediction model to verify the prediction performance at the sites of the aforementioned 10 cities. The statistical model can be used through four steps. First, establish a statistical linear regression model between the daily $PM_{2.5}$ concentrations and the previous day's ASI_{TS} values using data from 1 April 2013 to 31 March 2015 (i.e., the first 2 years) for every city site. Second, define an EHD as the day having extreme 5% high daily $PM_{2.5}$ concentrations during the first 2 years (the same as the definition in section 3b). The lower limits of the daily $PM_{2.5}$ concentrations on EHDs (denoted as $PM_{2.5}$-EHD) in the 10 cities are shown in Table 2. Third, calculate the previous day's ASI_{TS} values corresponding to $PM_{2.5}$-EHD using the linear regression model (Table 2, denoted as ASI_{TS}-PD). Fourth, apply the ASI_{TS}-PD results to the period from 1 April 2015 to 31 March 2016 (i.e., the last year), to predict the occurrences of EHDs and calculate the prediction accuracy (Table 2), which is defined as

$$\frac{\text{No. of EHDs with the previous day's } ASI_{TS} \geq ASI_{TS}\text{-PD}}{\text{No. of EHDs}} \times 100\%. \quad (9)$$

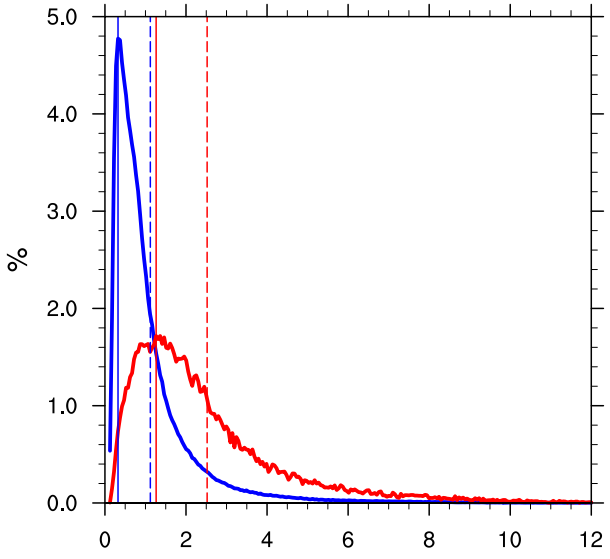

FIG. 6. ASI_{TS} PDFs on EHDs (red thick line; defined as days with daily $PM_{2.5}$ concentrations $>142\,\mu g\,m^{-3}$) and non-EHDs (blue thick line; defined as days with daily $PM_{2.5}$ concentrations $\leq 142\,\mu g\,m^{-3}$) between 1 Apr 2013 and 31 Mar 2016 in NC. The red (blue) thin line represents the ASI_{TS} values of the most likely ASI_{TS} on EHDs (non-EHDs). The red (blue) dashed line represents the mean ASI_{TS} values on EHDs (non-EHDs).

Taking Beijing for example, an EHD is defined by a daily $PM_{2.5}$ concentration $\geq 217.4\,\mu g\,m^{-3}$ Correspondingly, the previous day's ASI_{TS} value of an EHD would be greater than 1.9. Using such predictions by ASI_{TS} in the previous day, 72.7% (16 of 22 days) of the EHD can be captured in Beijing. In the other cities, the $PM_{2.5}$-EHD values were $103.9–300.3\,\mu g\,m^{-3}$, with the ASI_{TS}-PD values ranging from 1.7 to 3.9. The EHD prediction accuracies using ASI_{TS}-PD were 44.4%–100.0% in the 10 cities. The highest prediction accuracy was located in Shijiazhuang, which was also the most polluted among the 10 cities, with a $PM_{2.5}$-EHD of $300.3\,\mu g\,m^{-3}$. With this approach, although the ASI_{TS} scheme has no explicit consideration of emission, the ASI_{TS} prediction should also have an adjustment to the emission change to some degree, because the observed $PM_{2.5}$ concentrations in the recent 2 years are always used to build the statistical prediction model. Hence, if the emissions change in recent years, the $PM_{2.5}$ concentrations and the ASI_{TS}-PD can also have a corresponding adjustment. To summarize, we can predict all the occurrences of EHDs in Shijiazhuang over the last year using data from the previous 2 years only. The ASI_{TS} represents an easily used and computationally efficient method for EHD predictions, which could be a supplement to the CTM predictions in NC (see Table S2 in the online supplementary material). At last, it should be noted that this approach would not be favorable when the emissions substantially change in a very short term (such as several days), which is beyond the consideration of the statistical prediction model.

d. ASI_{TS} with low- and high-frequency signals of $PM_{2.5}$ concentrations

Many previous studies emphasized that changes in synoptic patterns are important drivers for variations in the $PM_{2.5}$ concentrations and the occurrences of aerosol pollution events in NC (Ye et al. 2016; Bei et al. 2016; Zheng et al. 2015; Y. Zhang et al. 2016). Modulating by such synoptic activity, the $PM_{2.5}$ concentrations have a strong cycle with a period of 4–7 days in NC (Guo et al. 2014; Quan et al. 2014, 2015). Synoptic activities can impact the variations in $PM_{2.5}$ concentrations via controlling the air stagnation conditions (Ye et al. 2016). Driven by favorable synoptic system activities, a stagnation weather pattern could last for several days (Wang and Angell 1999). Hence, in addition to monthly and daily time scales, it is necessary to study the relationship between ASI_{TS} and $PM_{2.5}$ concentration variations over a period of several days.

In this manuscript, we define low-frequency (high frequency) variations as a period greater than or equal to (less than) 5 days. Figure 9 shows the low-pass and high-pass $PM_{2.5}$ concentrations and the ASI_{TS} values for Beijing. The low- and high-pass signals are calculated using a Lanczos filter (Duchon 1979). It is shown that the relationship between ASI_{TS} and the $PM_{2.5}$ concentrations was more significant in the low-frequency variations than in the high-frequency variations. The low-frequency ASI_{TS} series was able to capture the crests and troughs of the $PM_{2.5}$ concentrations, especially for the episodes with high $PM_{2.5}$ concentrations in the wintertime. The simultaneous and largest lead–lag correlation coefficients in the low-frequency variations were 0.61 and 0.68, respectively (the largest lead–lag correlation was also observed when the ASI_{TS} led the $PM_{2.5}$ concentrations by 1 day, as shown in Fig. 7). By comparison, the high-frequency ASI_{TS} series was not clearly related to the variations in the $PM_{2.5}$ concentrations. The simultaneous correlation in the high-frequency series was not as significant as that in the low-frequency series. Although the lead–lag correlation coefficient for ASI_{TS} that led the $PM_{2.5}$ concentrations by 1 day passed the t test with 99% confidence, the correlation value was only 0.33, which was far smaller than the corresponding value of low-frequency series. The same results can also be seen in other cities in NC (see Figs. S1–S9 in the supplementary material). The results indicate that the influence of ASI_{TS} on the variations in the $PM_{2.5}$ concentrations mainly reflects the impacts of cycles of activity in synoptic systems, which has been reported in previous studies (Guo et al. 2014;

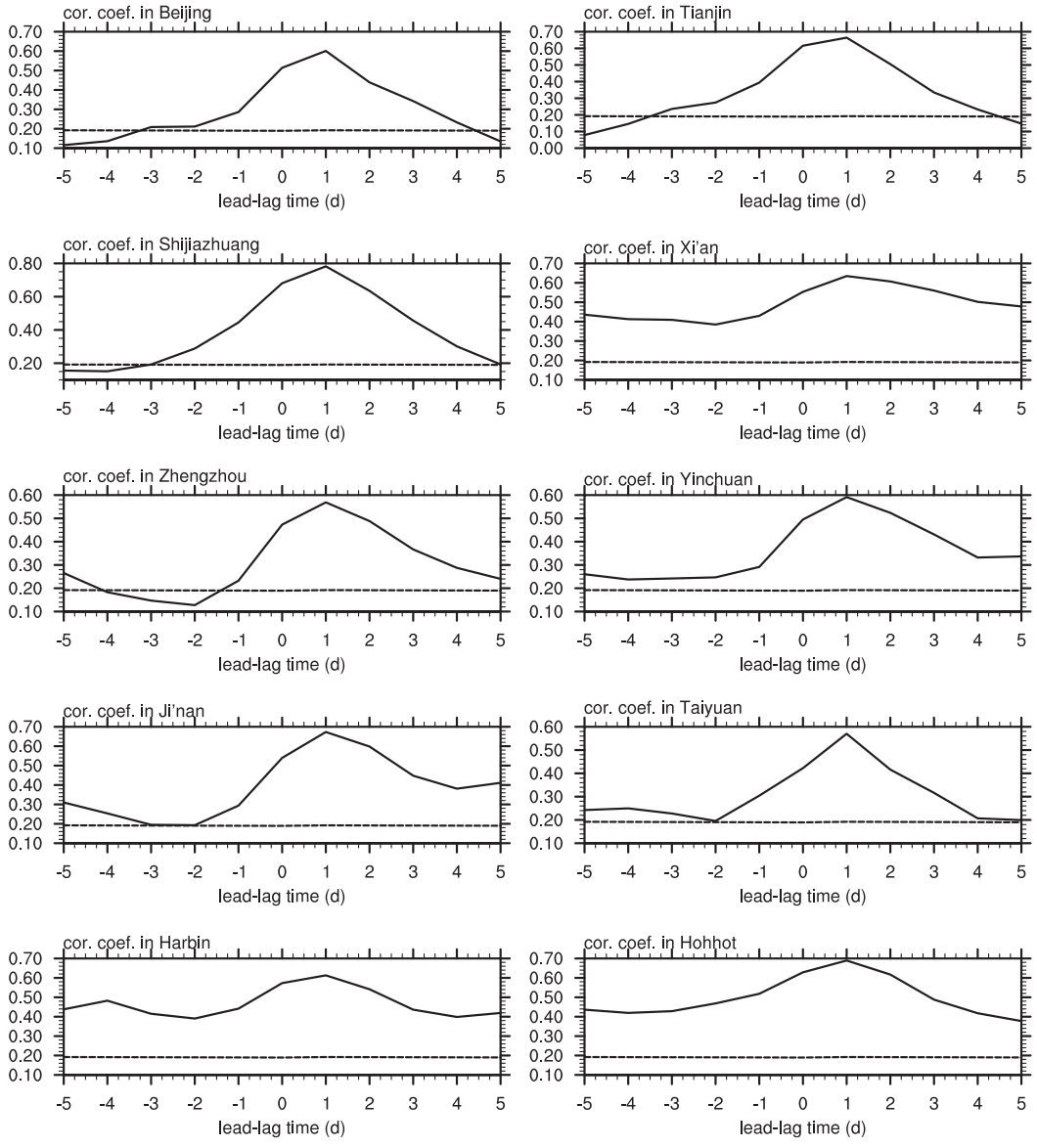

FIG. 7. Lead–lag correlation coefficients between the $PM_{2.5}$ concentrations and ASI_{TS} in the 10 aerosol-polluted cities in Figs. 4a and 5 between 1 Apr 2015 and 31 Mar 2016. The positive (negative) x-axis values denote the ASI_{TS} lead corresponding to the $PM_{2.5}$ concentrations ranging from −5 to 5 days. In particular, a value of 0 on the x axis denotes a simultaneous correlation. The dashed curves denote the t test at a 99% confidence level.

Quan et al. 2014, 2015). In addition, since the ASI_{TS} mainly reflects the variations in the $PM_{2.5}$ concentrations on synoptic time scales, it could also be used to assess the extreme haze events persisting for several days (see Table S1 in the supplementary material).

e. Sensitivity of the ASI_{TS} scheme to its parameters

Although the abovementioned results demonstrate that the new ASI_{TS} scheme in this manuscript is strongly related to the $PM_{2.5}$ concentrations in NC, the power-law exponent $\alpha = 1/4$ that we set in (4) and (8) is mainly based on the analysis of the order of magnitude. Therefore, it is necessary to analyze the sensitivity of the ASI_{TS} scheme to the parameter α. We calculate the monthly ASI_{TS} by adopting four different values of α equal to 1, 1/2, 1/3, and 1/5, and compute the correlation coefficients between the $PM_{2.5}$ concentrations and those ASI_{TS} series (Fig. 10). When $\alpha = 1/4$, the correlation coefficients are significant throughout most of NC. However, when α is set to 1, the correlation coefficients of most of the aerosol-polluted areas such as BTH are evidently smaller than the values when α is set to 1/4, as

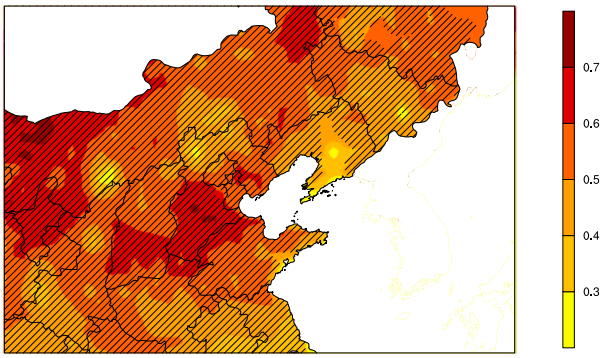

FIG. 8. As in Fig. 4a, but for the leading correlation coefficients between ASI_{TS} and the $PM_{2.5}$ concentrations at a lead of 1 day. The hatched areas denote the areas in which the lead correlation coefficients are greater than the simultaneous correlation coefficients shown in Fig. 4a.

shown in Fig. 1c. When α is set to 1/2, 1/3, and 1/5, the geopotential patterns of the correlation coefficients between the $PM_{2.5}$ concentrations and ASI_{TS} are very similar to those when α is set to 1/4. For example, in BTH, the correlation coefficients reached 0.8–0.9, 0.8–0.9, and 0.9–1.0 when α is equal to 1/2, 1/3, and 1/5, respectively. It is thus evident that α is not a sensitive parameter to the relationship between the stagnation conditions and the $PM_{2.5}$ concentrations in NC when $\alpha \leq 1/2$. The ASI_{TS} scheme adopted in this manuscript can efficiently reflect its relationship with variations in $PM_{2.5}$ concentrations.

Another noteworthy parameter in the ASI_{TS} is the PBLH since the PBLH could have much uncertainty due to various diagnosis methods and data (Von Engeln and Teixeira 2013; W. Zhang et al. 2016; Y. Zhang et al. 2014; Seidel et al. 2010; McGrath-Spangler and Molod 2014). To estimate the impacts of the uncertainty in PBLH, we calculated the daily ASI_{TS} when PBLH have random relative error less than 25% and 50%, respectively (Table 3). It is found that the ASI_{TS} with 25% and 50% uncertainty of PBLH were significantly correlated with the ASI_{TS} used in the manuscript, with the correlation coefficients of 0.98 and 0.91, respectively, and with the small normalized mean biases of 13% and 29%, respectively. Additionally, the PBLH directly from the reanalysis datasets should not be suitable for the real-time diagnosis of ASI_{TS} and haze prediction. So in this case, PBLH derived from other methods such as critical bulk Richardson number (BRN; McGrath-Spangler and Molod 2014; Guo et al. 2016; Y. Zhang et al. 2014) could also be used to calculate ASI_{TS} (see Fig. S10 in the supplementary material).

At last, we analyzed the uncertainty of ASI_{TS} induced by precipitation threshold by comparing the ASI_{TS} with the counterparts using the thresholds of 2 and 5 mm day^{-1}, respectively. It is also shown that the threshold of precipitation could not affect the ASI_{TS} values so much (Table 4).

4. Conclusions and discussion

This study introduced a new ASI_{TS} scheme to quantify the air stagnation conditions and investigate the relationship between ASI_{TS} and observed $PM_{2.5}$ concentrations on monthly and daily time scales. The new ASI_{TS} scheme considers air diffusion potency via advection, turbulence potency in the PBL, and the effect of wet deposition. The ASI_{TS} scheme was then applied to analyze and predict the occurrence of extreme haze events in NC between 1 April 2013 and 31 March 2016 using MERRA-2 meteorological fields and MEP/EMC $PM_{2.5}$ concentrations in NC.

ASI_{TS} showed a close relationship with the monthly variations and PDF of the $PM_{2.5}$ concentrations in NC. The correlation coefficients among 99.1% of the areas in NC passed the t test at a 99% confidence level. In many aerosol-polluted areas of NC, the correlation coefficients between ASI_{TS} and the $PM_{2.5}$ concentrations

TABLE 2. Lower limit of daily $PM_{2.5}$ concentrations on EHDs ($PM_{2.5}$-EHD), corresponding lower limits of ASI_{TS} on the previous day (ASI_{TS}-PD) calculated using data from 1 Apr 2013 to 31 Mar 2014, and prediction accuracies for EHDs using ASI_{TS} from 1 Apr 2015 to 31 Mar 2016 for the 10 cities in NC.

City	$PM_{2.5}$-EHD ($\mu g\ m^{-3}$)	ASI_{TS}-PD	Prediction accuracy (%)
Beijing	217.4	1.9	72.7 (16 of 22 days)
Tianjin	187.2	2.5	81.8 (9 of 11 days)
Shijiazhuang	300.3	2.1	100.0 (8 of 8 days)
Xi'an	189.0	1.5	80.0 (8 of 10 days)
Zhengzhou	202.9	2.0	88.2 (15 of 17 days)
Yinchuan	103.9	2.6	44.4 (12 of 27 days)
Ji'nan	183.8	2.1	75.0 (18 of 24 days)
Taiyuan	149.5	1.7	90.0 (9 of 10 days)
Harbin	211.0	3.9	58.3 (7 of 12 days)
Hohhot	113.9	1.8	77.3 (17 of 22 days)

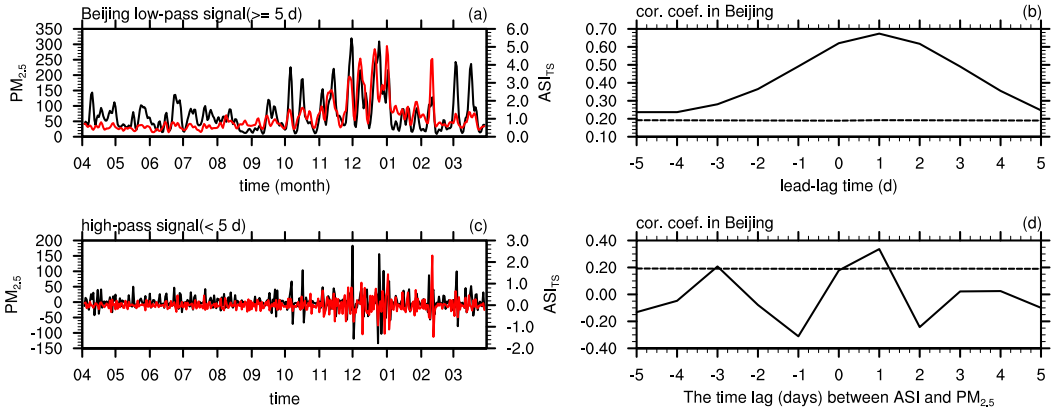

FIG. 9. (a) Low-pass and (c) high-pass $PM_{2.5}$ concentrations (black lines) and ASI_{TS} (red lines) and the corresponding lead–lag correlation coefficients between the (b) low-pass $PM_{2.5}$ concentrations and ASI_{TS} and the (d) high-pass $PM_{2.5}$ concentrations and ASI_{TS} in Beijing between 1 Mar 2015 and 31 Mar 2016. The positive and negative x-axis values for (b) and (d) denote the ASI_{TS} lead and lag correlation coefficients, respectively, corresponding to the $PM_{2.5}$ concentrations. The dashed curves denote the t test at a 99% confidence level.

reached 0.8–1.0. The PDFs of the monthly ASI_{TS} values and $PM_{2.5}$ concentrations in NC all showed lognormal distributions with similar NMBs. On the daily time scale, ASI_{TS} is applicable for analyzing the variations in the $PM_{2.5}$ concentrations and extreme haze events in NC. The daily ASI_{TS} and $PM_{2.5}$ in NC were significantly correlated from 1 April 2013 to 31 March 2016. The ASI_{TS} scheme was able to track the variations in the

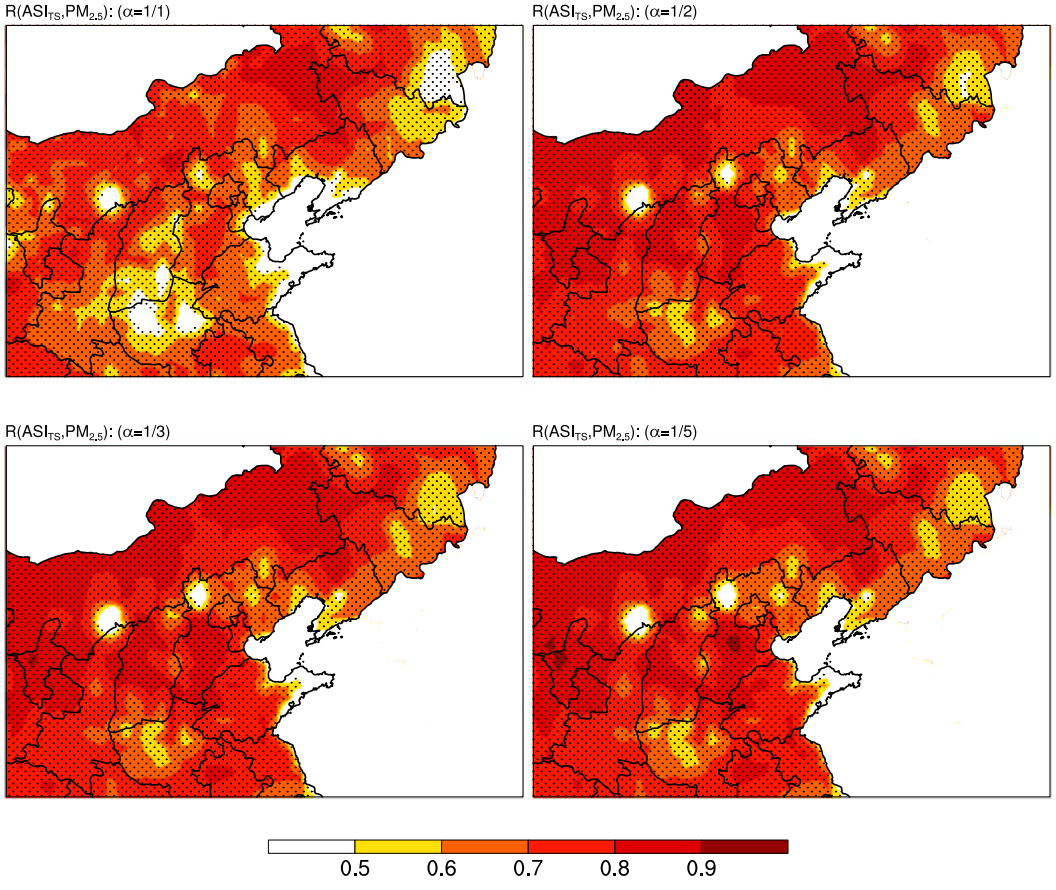

FIG. 10. As in Fig. 1c, but for the parameters $\alpha = 1, 1/2, 1/3$, and $1/5$ in (8).

TABLE 3. The correlation coefficients and NMB between the daily ASI_{TS} in the manuscript and the ASI_{TS} calculated by PBLH with uncertainties of 25% and 50% in NC from 1 Apr 2013 to 31 Mar 2016.

Uncertainty of PBLH (%)	Correlation coefficients of ASI_{TS}	NMB of ASI_{TS} (%)
25	0.98	13
50	0.91	29

TABLE 4. The correlation coefficients and NMB between the daily ASI_{TS} used in the manuscript and the ASI_{TS} calculated by the thresholds of 2 and 5 mm day^{-1} precipitation in NC from 1 Apr 2013 to 31 Mar 2016.

Threshold of precipitation (mm day^{-1})	Correlation coefficients of ASI_{TS}	NMB of ASI_{TS} (%)
2	0.99	3
5	0.97	7

$PM_{2.5}$ concentrations in the 10 polluted cities in NC. In addition, because the correlation coefficients for ASI_{TS} leading the $PM_{2.5}$ concentrations by 1 day were greater than the simultaneous correlation coefficients for approximately 98% of the grid cells of NC, ASI_{TS} is a useful leading predictor of the extreme haze events in NC. The prediction accuracies of extreme haze days using the ASI_{TS} scheme were favorably 44.4%–100.0% for the 10 cities. It is also found that the air stagnation conditions represented by ASI_{TS} and the $PM_{2.5}$ concentrations mainly depended on low-frequency variations (signal period $\geq$5 days) compared with high-frequency variations (signal period <5 days). These results indicate that the influence of ASI_{TS} on the variations in $PM_{2.5}$ concentrations mainly reflects the impacts of activities in synoptic systems, as was reported in previous studies.

It should be noted that this study only applied the ASI_{TS} scheme to NC. But we find that ASI_{TS} does not have a comparably strong relationship with the variations in the $PM_{2.5}$ concentrations over southern China (SC) as it does for NC. This could be possibly attributed to two reasons: 1) some parameters of ASI_{TS} are designed mainly with regard to the magnitudes of the variables for NC, and 2) other meteorological parameters, including higher humidity, temperature, and volatile organic compound emissions, are quite different in SC (Fu and Liao 2012) and are not related to the air stagnation conditions but could markedly impact the aerosol concentrations over SC (Li et al. 2014; Jiang et al. 2012; Y. W. Zhang et al. 2015; Chan et al. 2017; Qin et al. 2016; Jiang et al. 2008). Hence, a modified meteorology index involving additional physical and chemical processes is required to qualify EHDs and variations in the aerosol concentrations for SC.

Because of the good performance in illustrating the variations in the $PM_{2.5}$ concentrations driven by air stagnation weather, the ASI_{TS} scheme may be a useful tool for analyzing variations in the aerosol pollution in NC that are driven by variations in meteorological conditions on the synoptic scale and month-to-month time scale. Because of the significant leading correlations shown between the daily ASI_{TS} values and the $PM_{2.5}$ concentrations and simple calculation requirements, the ASI_{TS} scheme can be used to predict the occurrences of EHDs in NC. In section 3c, we simply used an empirical model with a constant ASI_{TS}-PD by the data of the first 2 years to predict the occurrences of EHDs in the third year. In practice, the ASI_{TS} and $PM_{2.5}$ data in the previous year can be used to establish a dynamically updated ASI_{TS}-PD and then to make a more favorable prediction. We think the ASI_{TS}-based prediction is just a supplementary tool for extreme haze event prediction and analysis in NC. For example, the ASI_{TS} could be a useful analysis tool to understand the causes of haze event occurrence in NC. By comparing with the ASI and CTM prediction, more could be understood about the effects of emissions and meteorology, respectively, in an extreme haze event. The ASI_{TS} prediction could also combine with the regional meteorological models and regional air quality models to forecast the extreme haze in the subsequent few days. Finally, because of the good relationship between monthly ASI_{TS} and $PM_{2.5}$ concentrations and the simple expressions of ASI_{TS}, the ASI_{TS} could be helpful for understanding the impacts of climate change and general atmospheric circulation on long-term variations in haze events over NC, which is one of the frontier study issues (Feng et al. 2016; Cai et al. 2017; Chen and Wang 2015; Ding and Liu 2014).

Acknowledgments. This work was supported by the National Natural Science Foundation of China (Grants 41705135 and 41575010), the Major Research Plan of the National Natural Science Foundation of China (Grant 91544219), and the Ministry of Science and Technology of China (Grant IUMKY201620).

REFERENCES

Bei, N., and Coauthors, 2016: Typical synoptic situations and their impacts on the wintertime air pollution in the Guanzhong basin, China. *Atmos. Chem. Phys.*, **16**, 7373–7387, https://doi.org/10.5194/acp-16-7373-2016.

Bosilovich, M. G., and Coauthors, 2015: MERRA-2 : Initial evaluation of the climate. NASA Tech. Memo. NASA/TM-2015-104606/Vol. 43, 145 pp., https://gmao.gsfc.nasa.gov/pubs/docs/Bosilovich803.pdf.

——, F. R. Robertson, L. Takacs, A. Molod, and D. Mocko, 2017: Atmospheric water balance and variability in the MERRA-2

reanalysis. *J. Climate*, **30**, 1177–1196, https://doi.org/10.1175/JCLI-D-16-0338.1.

Cai, W., K. Li, H. Liao, H. Wang, and L. Wu, 2017: Weather conditions conducive to Beijing severe haze more frequent under climate change. *Nat. Climate Change*, **7**, 257–262, https://doi.org/10.1038/nclimate3249.

Chan, K. L., S. Wang, C. Liu, B. Zhou, M. O. Wenig, and A. Saiz-Lopez, 2017: On the summertime air quality and related photochemical processes in the megacity Shanghai, China. *Sci. Total Environ.*, **580**, 974–983, https://doi.org/10.1016/j.scitotenv.2016.12.052.

Chen, C., and Coauthors, 2015: Characteristics and sources of submicron aerosols above the urban canopy (260 m) in Beijing, China, during the 2014 APEC summit. *Atmos. Chem. Phys.*, **15**, 12 879–12 895, https://doi.org/10.5194/acp-15-12879-2015.

Chen, D., Z. Liu, J. Fast, and J. Ban, 2016: Simulations of sulfate–nitrate–ammonium (SNA) aerosols during the extreme haze events over northern China in October 2014. *Atmos. Chem. Phys.*, **16**, 10 707–10 724, https://doi.org/10.5194/acp-16-10707-2016.

Chen, H., and H. Wang, 2015: Haze days in north China and the associated atmospheric circulations based on daily visibility data from 1960 to 2012. *J. Geophys. Res. Atmos.*, **120**, 5895–5909, https://doi.org/10.1002/2015JD023225.

Chen, J., and Coauthors, 2012: A parameterization of low visibilities for hazy days in the North China Plain. *Atmos. Chem. Phys.*, **12**, 4935–4950, https://doi.org/10.5194/acp-12-4935-2012.

Chen, Z., J. Zhang, T. Zhang, W. Liu, and J. Liu, 2015: Haze observations by simultaneous lidar and WPS in Beijing before and during APEC, 2014. *Sci. China Chem.*, **58**, 1385–1392, https://doi.org/10.1007/s11426-015-5467-x.

Cobourn, W. G., 2010: An enhanced $PM_{2.5}$ air quality forecast model based on nonlinear regression and back-trajectory concentrations. *Atmos. Environ.*, **44**, 3015–3023, https://doi.org/10.1016/j.atmosenv.2010.05.009.

Coy, L., K. Wargan, A. M. Molod, W. R. McCarty, and S. Pawson, 2016: Structure and dynamics of the quasi-biennial oscillation in MERRA-2. *J. Climate*, **29**, 5339–5354, https://doi.org/10.1175/JCLI-D-15-0809.1.

Ding, Y., and Y. Liu, 2014: Analysis of long-term variations of fog and haze in China in recent 50 years and their relations with atmospheric humidity. *Sci. China Earth Sci.*, **57**, 36–46, https://doi.org/10.1007/s11430-013-4792-1.

Duchon, C. E., 1979: Lanczos filtering in one and two dimensions. *J. Appl. Meteor.*, **18**, 1016–1022, https://doi.org/10.1175/1520-0450(1979)018<1016:LFIOAT>2.0.CO;2.

Feng, J., H. Liao, and Y. Gu, 2016: A comparison of meteorology-driven interannual variations of surface aerosol concentrations in the eastern United States, eastern China, and Europe. *SOLA*, **12**, 146–152, https://doi.org/10.2151/sola.2016-031.

Fu, Y., and H. Liao, 2012: Simulation of the interannual variations of biogenic emissions of volatile organic compounds in China: Impacts on tropospheric ozone and secondary organic aerosol. *Atmos. Environ.*, **59**, 170–185, https://doi.org/10.1016/j.atmosenv.2012.05.053.

Gao, M., G. R. Carmichael, P. E. Saide, Z. Lu, M. Yu, D. G. Streets, and Z. Wang, 2016: Response of winter fine particulate matter concentrations to emission and meteorology changes in north China. *Atmos. Chem. Phys.*, **16**, 11 837–11 851, https://doi.org/10.5194/acp-16-11837-2016.

Gelaro, R., and Coauthors, 2017: The Modern-Era Retrospective Analysis for Research and Applications, version 2 (MERRA-2). *J. Climate*, **30**, 5419–5454, https://doi.org/10.1175/JCLI-D-16-0758.1.

Gui, K., and Coauthors, 2016: Aerosol optical properties based on ground and satellite retrievals during a serious haze episode in December 2015 over Beijing. *Atmosphere*, **7**, 70, https://doi.org/10.3390/atmos7050070.

Guo, H., Y. Wang, and H. Zhang, 2017: Characterization of criteria air pollutants in Beijing during 2014–2015. *Environ. Res.*, **154**, 334–344, https://doi.org/10.1016/j.envres.2017.01.029.

Guo, J., and Coauthors, 2016: The climatology of planetary boundary layer height in China derived from radiosonde and reanalysis data. *Atmos. Chem. Phys.*, **16**, 13 309–13 319, https://doi.org/10.5194/acp-16-13309-2016.

Guo, L., X. Guo, C. Fang, and S. Zhu, 2015: Observation analysis on characteristics of formation, evolution and transition of a long-lasting severe fog and haze episode in north China. *Sci. China Earth Sci.*, **58**, 329–344, https://doi.org/10.1007/s11430-014-4924-2.

Guo, S., and Coauthors, 2014: Elucidating severe urban haze formation in China. *Proc. Natl. Acad. Sci. USA*, **111**, 17 373–17 378, https://doi.org/10.1073/pnas.1419604111.

Han, S., and Coauthors, 2014: Characteristics and formation mechanism of a winter haze—Fog episode in Tianjin, China. *Atmos. Environ.*, **98**, 323–330, https://doi.org/10.1016/j.atmosenv.2014.08.078.

Hara, Y., and Coauthors, 2011: Seasonal characteristics of spherical aerosol distribution in eastern Asia: Integrated analysis using ground/space-based lidars and a chemical transport model. *SOLA*, **7**, 121–124, https://doi.org/10.2151/sola.2011-031.

He, Q., C. Li, F. Geng, G. Zhou, W. Gao, W. Yu, Z. Li, and M. Du, 2016: A parameterization scheme of aerosol vertical distribution for surface-level visibility retrieval from satellite remote sensing. *Remote Sens. Environ.*, **181**, 1–13, https://doi.org/10.1016/j.rse.2016.03.016.

Horton, D. E., Harshvardhan, and N. S. Diffenbaugh, 2012: Response of air stagnation frequency to anthropogenically enhanced radiative forcing. *Environ. Res. Lett.*, **7**, 044034, https://doi.org/10.1088/1748-9326/7/4/044034.

——, C. B. Skinner, D. Singh, and N. S. Diffenbaugh, 2014: Occurrence and persistence of future atmospheric stagnation events. *Nat. Climate Change*, **4**, 698–703, https://doi.org/10.1038/nclimate2272.

Hu, J., Y. Wang, Q. Ying, and H. Zhang, 2014: Spatial and temporal variability of $PM_{2.5}$ and PM_{10} over the North China Plain and the Yangtze River delta, China. *Atmos. Environ.*, **95**, 598–609, https://doi.org/10.1016/j.atmosenv.2014.07.019.

——, J. Chen, Q. Ying, and H. Zhang, 2016: One-year simulation of ozone and particulate matter in China using WRF/CMAQ modeling system. *Atmos. Chem. Phys.*, **16**, 10 333–10 350, https://doi.org/10.5194/acp-16-10333-2016.

Huang, L., C.-S. Yuan, G. Wang, and K. Wang, 2011: Chemical characteristics and source apportionment of PM_{10} during a brown haze episode in Harbin, China. *Particuology*, **9**, 32–38, https://doi.org/10.1016/j.partic.2010.07.022.

Huang, Q., X. Cai, Y. Song, and T. Zhu, 2017: Air stagnation in China (1985–2014): Climatological mean features and trends. *Atmos. Chem. Phys.*, **17**, 7793–7805, https://doi.org/10.5194/acp-17-7793-2017.

IPCC, 2013: *Climate Change 2013: The Physical Science Basis*. Cambridge University Press, 1535 pp., https://doi.org/10.1017/CBO9781107415324.

Jacob, D. J., and D. A. Winner, 2009: Effect of climate change on air quality. *Atmos. Environ.*, **43**, 51–63, https://doi.org/10.1016/j.atmosenv.2008.09.051.

Jiang, F., T. Wang, T. Wang, M. Xie, and H. Zhao, 2008: Numerical modeling of a continuous photochemical pollution episode in

Hong Kong using WRF–Chem. *Atmos. Environ.*, **42**, 8717–8727, https://doi.org/10.1016/j.atmosenv.2008.08.034.

——, Q. Liu, X. Huang, T. Wang, B. Zhuang, and M. Xie, 2012: Regional modeling of secondary organic aerosol over China using WRF/Chem. *J. Aerosol Sci.*, **43**, 57–73, https://doi.org/10.1016/j.jaerosci.2011.09.003.

Jiang, Y., R. Zhu, K. Zhu, and Z. Li, 2015: Numerical simulation on the air pollution potential in the severe air pollution episodes in Beijing–Tianjin–Hebei region (in Chinese). *Acta Sci. Circumstantiae*, **35**, 2681–2692.

Korshover, J., 1976: Climatology of stagnating anticyclones east of the Rocky Mountains, 1936–1975. NOAA Tech. Memo. ERL ARL-55, 26 pp.

——, and J. K. Angell, 1982: A review of air-stagnation cases in the eastern United States during 1981—Annual summary. *Mon. Wea. Rev.*, **110**, 1515–1518, https://doi.org/10.1175/1520-0493(1982)110<1515:AROASC>2.0.CO;2.

Koster, R. D., and Coauthors, 2016: MERRA-2 input observations: Summary and assessment. NASA/TM-2016-104606/Vol. 46, 51 pp., https://ntrs.nasa.gov/archive/nasa/casi.ntrs.nasa.gov/20160014544.pdf.

Leibensperger, E. M., L. J. Mickley, and D. J. Jacob, 2008: Sensitivity of US air quality to mid-latitude cyclone frequency and implications of 1980–2006 climate change. *Atmos. Chem. Phys.*, **8**, 7075–7086, https://doi.org/10.5194/acpd-8-12253-2008.

Li, J., and Z. Han, 2016: Aerosol vertical distribution over east China from RIEMS-Chem simulation in comparison with CALIPSO measurements. *Atmos. Environ.*, **143**, 177–189, https://doi.org/10.1016/j.atmosenv.2016.08.045.

Li, J., H. Du, Z. Wang, Y. Sun, W. Yang, J. J. Li, X. Tang, and P. Fu, 2017: Rapid formation of a severe regional winter haze episode over a mega-city cluster on the North China Plain. *Environ. Pollut.*, **223**, 605–615, https://doi.org/10.1016/j.envpol.2017.01.063.

Li, L., and Coauthors, 2014: An integrated process rate analysis of a regional fine particulate matter episode over Yangtze River delta in 2010. *Atmos. Environ.*, **91**, 60–70, https://doi.org/10.1016/j.atmosenv.2014.03.053.

Li, Z., and Coauthors, 2016: Remote sensing of atmospheric particulate mass of dry $PM_{2.5}$ near the ground: Method validation using ground-based measurements. *Remote Sens. Environ.*, **173**, 59–68, https://doi.org/10.1016/j.rse.2015.11.019.

——, and Coauthors, 2017: Aerosol and boundary-layer interactions and impact on air quality. *Natl. Sci. Rev.*, **4**, 810–833, https://doi.org/10.1093/nsr/nwx117.

Lin, J.-T., and M. B. McElroy, 2010: Impacts of boundary layer mixing on pollutant vertical profiles in the lower troposphere: Implications to satellite remote sensing. *Atmos. Environ.*, **44**, 1726–1739, https://doi.org/10.1016/j.atmosenv.2010.02.009.

Liu, J., D. Wu, and S. J. Fan, 2015: Distribution of regional pollution and the characteristics of vertical wind field in the Pearl River delta (in Chinese). *Environ. Sci.*, **36**, 3989–3998.

Liu, Y., M. Franklin, R. Kahn, and P. Koutrakis, 2007: Using aerosol optical thickness to predict ground-level $PM_{2.5}$ concentrations in the St. Louis area: A comparison between MISR and MODIS. *Remote Sens. Environ.*, **107**, 33–44, https://doi.org/10.1016/j.rse.2006.05.022.

Long, X., and Coauthors, 2016: Impact of crop field burning and mountains on heavy haze in the North China Plain: A case study. *Atmos. Chem. Phys.*, **16**, 9675–9691, https://doi.org/10.5194/acp-16-9675-2016.

Lu, H.-C., 2002: The statistical characters of PM_{10} concentration in Taiwan area. *Atmos. Environ.*, **36**, 491–502, https://doi.org/10.1016/S1352-2310(01)00245-X.

Mamtimin, B., and F. X. Meixner, 2011: Air pollution and meteorological processes in the growing dryland city of Urumqi (Xinjiang, China). *Sci. Total Environ.*, **409**, 1277–1290, https://doi.org/10.1016/j.scitotenv.2010.12.010.

Mao, J., H. Sheng, H. Zhao, and C. Zhou, 2014: Observation study on the size distribution of sand dust aerosol particles over Yinchuan, China. *Adv. Meteor.*, **2014**, 157645, https://doi.org/10.1155/2014/157645.

McGrath-Spangler, E. L., and A. Molod, 2014: Comparison of GEOS-5 AGCM planetary boundary layer depths computed with various definitions. *Atmos. Chem. Phys.*, **14**, 6717–6727, https://doi.org/10.5194/acp-14-6717-2014.

Mijling, B., R. J. van der A, and Q. Zhang, 2013: Regional nitrogen oxides emission trends in East Asia observed from space. *Atmos. Chem. Phys.*, **13**, 12 003–12 012, https://doi.org/10.5194/acp-13-12003-2013.

Mu, Q., and H. Liao, 2014: Simulation of the interannual variations of aerosols in China: Role of variations in meteorological parameters. *Atmos. Chem. Phys.*, **14**, 11 177–11 219, https://doi.org/10.5194/acpd-14-11177-2014.

Ovadnevaitė, J., K. Kvietkus, and J. Šakalys, 2007: Evaluation of the impact of long-range transport and aerosol concentration temporal variations at the eastern coast of the Baltic Sea. *Environ. Monit. Assess.*, **132**, 365–375, https://doi.org/10.1007/s10661-006-9540-y.

Qin, Y. M., Y. J. Li, H. Wang, B. P. Y. L. Lee, D. D. Huang, and C. K. Chan, 2016: Particulate matter (PM) episodes at a suburban site in Hong Kong: Evolution of PM characteristics and role of photochemistry in secondary aerosol formation. *Atmos. Chem. Phys.*, **16**, 14 131–14 145, https://doi.org/10.5194/acp-16-14131-2016.

Quan, J., Q. Zhang, H. He, J. Liu, M. Huang, and H. Jin, 2011: Analysis of the formation of fog and haze in North China Plain (NCP). *Atmos. Chem. Phys.*, **11**, 8205–8214, https://doi.org/10.5194/acp-11-8205-2011.

——, X. Tie, Q. Zhang, Q. Liu, X. Li, Y. Gao, and D. Zhao, 2014: Characteristics of heavy aerosol pollution during the 2012–2013 winter in Beijing, China. *Atmos. Environ.*, **88**, 83–89, https://doi.org/10.1016/j.atmosenv.2014.01.058.

——, Q. Liu, X. Li, Y. Gao, X. Jia, J. Sheng, and Y. Liu, 2015: Effect of heterogeneous aqueous reactions on the secondary formation of inorganic aerosols during haze events. *Atmos. Environ.*, **122**, 306–312, https://doi.org/10.1016/j.atmosenv.2015.09.068.

Reichle, R. H., Q. Liu, R. D. Koster, C. S. Draper, S. P. P. Mahanama, and G. S. Partyka, 2017: Land surface precipitation in MERRA-2. *J. Climate*, **30**, 1643–1664, https://doi.org/10.1175/JCLI-D-16-0570.1.

Šakalys, J., K. Kvietkus, D. Čeburnis, and D. Valiulis, 2004: The method of determination of heavy metals background concentration in the moss. *Environ. Chem. Phys.*, **26**, 109–117.

Seidel, D. J., C. O. Ao, and K. Li, 2010: Estimating climatological planetary boundary layer heights from radiosonde observations: Comparison of methods and uncertainty analysis. *J. Geophys. Res.*, **115**, D16113, https://doi.org/10.1029/2009JD013680.

Seinfeld, J. H., and S. N. Pandis, 2006: *Atmospheric Chemistry and Physics: From Air Pollution to Climate Change.* 2nd ed. Wiley-Interscience, 1232 pp.

Sun, X., Y. Yin, Y. Sun, Y. Sun, W. Liu, and Y. Han, 2013: Seasonal and vertical variations in aerosol distribution over Shijiazhuang, China. *Atmos. Environ.*, **81**, 245–252, https://doi.org/10.1016/j.atmosenv.2013.08.009.

Tai, A. P. K., L. J. Mickley, and D. J. Jacob, 2010: Correlations between fine particulate matter ($PM_{2.5}$) and meteorological

variables in the United States: Implications for the sensitivity of $PM_{2.5}$ to climate change. *Atmos. Environ.*, **44**, 3976–3984, https://doi.org/10.1016/j.atmosenv.2010.06.060.

——, ——, ——, E. M. Leibensperger, L. Zhang, J. A. Fisher, and H. O. T. Pye, 2012: Meteorological modes of variability for fine particulate matter ($PM_{2.5}$) air quality in the United States: Implications for $PM_{2.5}$ sensitivity to climate change. *Atmos. Chem. Phys.*, **12**, 3131–3145, https://doi.org/10.5194/acp-12-3131-2012.

Tang, Y.-X., H. Liao, and J. Feng, 2017: Estimating emissions and concentrations of road dust aerosol over China using the GEOS-Chem model. *Atmos. Ocean. Sci. Lett.*, **10**, 298–305, https://doi.org/10.1080/16742834.2017.1320935.

Tie, X., D. Wu, and G. Brasseur, 2009: Lung cancer mortality and exposure to atmospheric aerosol particles in Guangzhou, China. *Atmos. Environ.*, **43**, 2375–2377, https://doi.org/10.1016/j.atmosenv.2009.01.036.

Von Engeln, A., and J. Teixeira, 2013: A planetary boundary layer height climatology derived from ECMWF reanalysis data. *J. Climate*, **26**, 6575–6590, https://doi.org/10.1175/JCLI-D-12-00385.1.

Wang, J. X. L., and J. K. Angell, 1999: Air stagnation climatology for the United States (1948-1998). NOAA/Air Resources Laboratory ATLAS 1, 76 pp., https://www.arl.noaa.gov/documents/reports/atlas.pdf.

Wang, S., S. Yu, P. Li, L. Wang, K. Mehmood, W. Liu, R. Yan, and X. Zheng, 2017: A study of characteristics and origins of haze pollution in Zhengzhou, China, based on observations and hybrid receptor models. *Aerosol Air Qual. Res.*, **17**, 513–528, https://doi.org/10.4209/aaqr.2016.06.0238.

Wang, X., and Coauthors, 2014: Severe haze episodes and seriously polluted fog water in Ji'nan, China. *Sci. Total Environ.*, **493**, 133–137, https://doi.org/10.1016/j.scitotenv.2014.05.135.

Wang, Y., A. Khalizov, M. Levy, and R. Zhang, 2013: New directions: Light absorbing aerosols and their atmospheric impacts. *Atmos. Environ.*, **81**, 713–715, https://doi.org/10.1016/j.atmosenv.2013.09.034.

——, Q. Q. Zhang, K. He, Q. Zhang, and L. Chai, 2013: Sulfate–nitrate–ammonium aerosols over China: Response to 2000–2015 emission changes of sulfur dioxide, nitrogen oxides, and ammonia. *Atmos. Chem. Phys.*, **13**, 2635–2652, https://doi.org/10.5194/acp-13-2635-2013.

Wang, Y. H., Z. R. Liu, J. K. Zhang, B. Hu, D. S. Ji, Y. C. Yu, and Y. S. Wang, 2015: Aerosol physicochemical properties and implications for visibility during an intense haze episode during winter in Beijing. *Atmos. Chem. Phys.*, **15**, 3205–3215, https://doi.org/10.5194/acp-15-3205-2015.

Yang, Y. Q., and Coauthors, 2016: PLAM—A meteorological pollution index for air quality and its applications in fog-haze forecasts in north China. *Atmos. Chem. Phys.*, **16**, 1353–1364, https://doi.org/10.5194/acp-16-1353-2016.

Yang, Y. R., and Coauthors, 2015: Characteristics and formation mechanism of continuous hazes in China: A case study during the autumn of 2014 in the North China Plain. *Atmos. Chem. Phys.*, **15**, 8165–8178, https://doi.org/10.5194/acp-15-8165-2015.

Ye, X., Y. Song, X. Cai, and H. Zhang, 2016: Study on the synoptic flow patterns and boundary layer process of the severe haze events over the North China Plain in January 2013. *Atmos. Environ.*, **124**, 129–145, https://doi.org/10.1016/j.atmosenv.2015.06.011.

You, W., Z. Zang, L. Zhang, Y. Li, and W. Wang, 2016: Estimating national-scale ground-level PM_{25} concentration in China using geographically weighted regression based on MODIS and MISR AOD. *Environ. Sci. Pollut. Res. Int.*, **23**, 8327–8338, https://doi.org/10.1007/s11356-015-6027-9.

Zhang, Q., and Coauthors, 2015: Variations in $PM_{2.5}$, TSP, BC, and trace gases (NO_2, SO_2, and O_3) between haze and non-haze episodes in winter over Xi'an, China. *Atmos. Environ.*, **112**, 64–71, https://doi.org/10.1016/j.atmosenv.2015.04.033.

Zhang, R., Q. Li, and R. Zhang, 2014: Meteorological conditions for the persistent severe fog and haze event over eastern China in January 2013. *Sci. China Earth Sci.*, **57**, 26–35, https://doi.org/10.1007/s11430-013-4774-3.

Zhang, T., W. Gong, W. Wang, Y. Ji, Z. Zhu, and Y. Huang, 2016: Ground level $PM_{2.5}$ estimates over China using satellite-based geographically weighted regression (GWR) models are improved by including NO_2 and enhanced vegetation index (EVI). *Int. J. Environ. Res. Public Health*, **13**, 1215, https://doi.org/10.3390/ijerph13121215.

Zhang, W., J. Guo, Y. Miao, H. Liu, Y. Zhang, Z. Li, and P. Zhai, 2016: Planetary boundary layer height from CALIOP compared to radiosonde over China. *Atmos. Chem. Phys.*, **16**, 9951–9963, https://doi.org/10.5194/acp-16-9951-2016.

Zhang, X. Y. C., Y. Q. Wang, T. Niu, S. L. Gong, Y. M. Zhang, and J. Y. Sun, 2012: Atmospheric aerosol compositions in China: Spatial/temporal variability, chemical signature, regional haze distribution and comparisons with global aerosols. *Atmos. Chem. Phys.*, **12**, 779–799, https://doi.org/10.5194/acp-12-779-2012.

Zhang, Y., and Z. Li, 2015: Remote sensing of atmospheric fine particulate matter ($PM_{2.5}$) mass concentration near the ground from satellite observation. *Remote Sens. Environ.*, **160**, 252–262, https://doi.org/10.1016/j.rse.2015.02.005.

——, Z. Gao, D. Li, Y. Li, N. Zhang, X. Zhao, and J. Chen, 2014: On the computation of planetary boundary-layer height using the bulk Richardson number method. *Geosci. Model Dev.*, **7**, 2599–2611, https://doi.org/10.5194/gmd-7-2599-2014.

——, A. Ding, H. Mao, W. Nie, D. Zhou, L. Liu, X. Huang, and C. Fu, 2016: Impact of synoptic weather patterns and interdecadal climate variability on air quality in the North China Plain during 1980–2013. *Atmos. Environ.*, **124**, 119–128, https://doi.org/10.1016/j.atmosenv.2015.05.063.

Zhang, Y. W., and Coauthors, 2015: Significant concentration changes of chemical components of PM_1 in the Yangtze River delta area of China and the implications for the formation mechanism of heavy haze–fog pollution. *Sci. Total Environ.*, **538**, 7–15, https://doi.org/10.1016/j.scitotenv.2015.06.104.

Zhao, T. L., S. L. Gong, P. Huang, and D. Lavoué, 2012: Hemispheric transport and influence of meteorology on global aerosol climatology. *Atmos. Chem. Phys.*, **12**, 7609–7624, https://doi.org/10.5194/acp-12-7609-2012.

Zhao, X. J., P. S. Zhao, J. Xu, W. Meng, W. W. Pu, F. Dong, D. He, and Q. F. Shi, 2013: Analysis of a winter regional haze event and its formation mechanism in the North China Plain. *Atmos. Chem. Phys.*, **13**, 5685–5696, https://doi.org/10.5194/acp-13-5685-2013.

Zheng, G. J., and Coauthors, 2015: Exploring the severe winter haze in Beijing: The impact of synoptic weather, regional transport and heterogeneous reactions. *Atmos. Chem. Phys.*, **15**, 2969–2983, https://doi.org/10.5194/acp-15-2969-2015.

Zou, B., J. Chen, L. Zhai, X. Fang, and Z. Zheng, 2017: Satellite based mapping of ground $PM_{2.5}$ concentration using generalized additive modeling. *Remote Sens.*, **9**, 1, https://doi.org/10.3390/rs9010001.